ChemSusChem

Supporting Information

Identification of Active Sites for CO_2 Reduction on Graphene-Supported Single-Atom Catalysts

Youngho Kang,* Sungwoo Kang, and Seungwu Han

Table S1. ZPE, −TS, and DFT energy of gas species. The gas-phase corrected energy for CO_2 is given in the parenthesis.

	ZPE (eV)	−TS (eV)	Energy (eV)
H_2	0.27	−0.42	−6.98
CO	0.14	−0.61	−14.45
CO_2	0.31	−0.65	−22.32 (−21.87)
H_2O	0.57	−0.65	−14.15
CH_4	1.20	−0.59	−24.05

Table S2. ZPE, −TS, and DFT energy of adsorbates on the Zn site in a ZnN_4 moiety.

	ZPE (eV)	−TS (eV)	Energy (eV)
*OCHO	0.59	−0.22	−645.88
*COOH	0.59	−0.22	−645.14
*OCHOH	0.91	−0.30	−649.41
*CHO	0.43	−0.17	−637.44

Table S3. ZPE, −TS, and DFT energy of adsorbates on the Zn site in a ZnN_3C moiety.

	ZPE (eV)	−TS (eV)	Energy (eV)
*OCHO	0.59	−0.31	-645.16
*COOH	0.58	−0.24	-644.34

Table S4. ZPE, −TS, and DFT energy of adsorbates on the C_{NN} site in a ZnN_3C moiety. When *OCHO and *OCHOH are present on the neighboring Zn site, the adsorbed COOH is denoted as *COOH[a] and *COOH[b], respectively. *COOH[c] indicates the adsorbed COOH in a N_3C moiety.

	ZPE (eV)	−TS (eV)	Energy (eV)
*COOH	0.65	−0.19	−645.16
*COOH[a]	0.65	−0.17	−671.12
*COOH[b]	0.65	−0.18	−674.94
*COOH[c]	0.66	−0.18	−643.17
*CO	0.24	−0.13	−633.23
*CHO	0.52	−0.12	−638.08
*CHOH	0.86	−0.13	−641.55
*CH_2OH	1.13	−0.14	−645.26
*CH_2	0.73	−0.04	−634.94
*CH_3	1.03	−0.09	−639.19

Figure S1. Binding energies of Zn on a divacancy site in N_xC_{4-x} moieties.

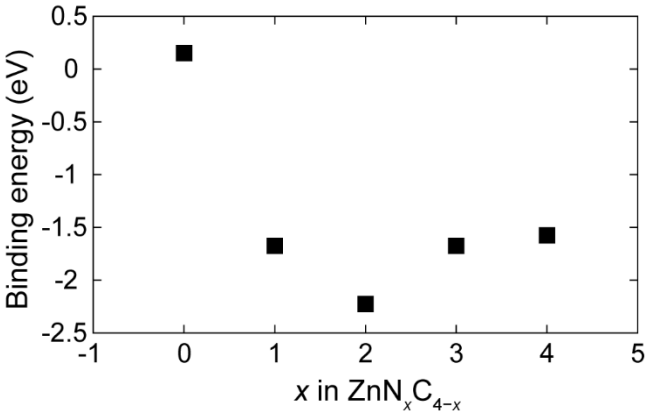

The binding energy E_b is calculated as follows:

$$E_b = E_{\mathrm{tot}}(\mathrm{ZnN}_x\mathrm{C}_{4-x}) - E_{\mathrm{tot}}(\mathrm{N}_x\mathrm{C}_{4-x}) - E_{\mathrm{tot}}(\mathrm{Zn}),$$

where $E_{\mathrm{tot}}(\mathrm{ZnN}_x\mathrm{C}_{4-x})$ and $E_{\mathrm{tot}}(\mathrm{N}_x\mathrm{C}_{4-x})$ are the DFT total energy of $\mathrm{ZnN}_x\mathrm{C}_{4-x}$ and $\mathrm{N}_x\mathrm{C}_{4-x}$ moieties, respectively. $E_{\mathrm{tot}}(\mathrm{Zn})$ is the energy per atom of the bulk Zn metal.

Figure S2. Potential CO_2R route to CH_4 on the C_{NN} site in a ZnN_3C moiety.

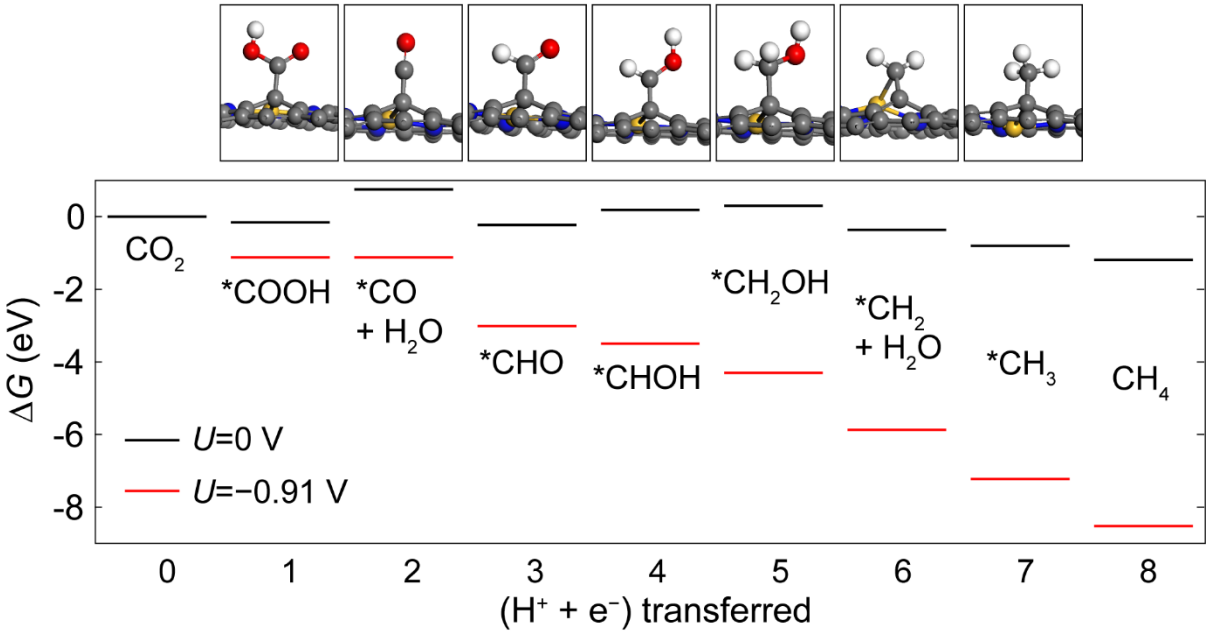

[Kinetic analysis]

We conducted CI-NEB calculations for kinetic analysis and determined potential-dependent kinetic barriers following the method used in previous works[1,2]. We focused on the first and second protonation steps on a C_{NN} site in a ZnN_3C moiety (Figure S3). Each protonation step corresponds to the electrochemical reaction of COOH and CO formation, respectively. Atomic configurations of initial (IS) and final states (FS) considered in the CI-NEB calculations and that of a transition state discovered are shown in Figure S4 for COOH formation and Figure S5 for CO formation. (In general, a CI-NEB calculation result depends on a specific reaction path and there may be other reaction routes that yield kinetic barriers smaller than those we obtained in Figure S3.) The DFT energy barriers in Figure S3 were converted into the free-energy barriers (E_a's) by applying a zero-point energy correction. Each CI-NEB result was assigned to the corresponding electrode potential U_0 at which the reaction of $A^* + H^+ + e^- \leftrightarrow A^* + H^*$, where A* is a reactant and H* is neutral hydrogen, is in equilibrium. When determining U_0, the free energy of a proton-electron pair was assumed to be equal to half of that of gaseous hydrogen at 1 atm. Thus, U_0 is referenced to RHE. To obtain E_a's at other potentials, Butler-Volmer theory was employed and a reaction symmetry factor β was set to 0.5±0.2 for simplicity; β is known to typically vary between 0.3 and 0.7.

From the CI-NEB calculations, we find that the E_a for the COOH formation is 0.14 eV at U_0=−0.85 V vs. RHE. Thus, at zero bias, the E_a is estimated to be 0.56(±0.17) eV. At U=−0.4 and −0.6 V vs. RHE at which Faraday efficiencies of CO_2R reach 80% in experiments, the E_a is reduced to 0.36(±0.09) and 0.26(±0.05) eV, respectively, compared to that at zero bias. Overall, together with the fact that the COOH formation is thermodynamically favorable, the small E_a's manifest the reason why Zn-N-G catalysts exhibit high Faraday efficiencies of CO_2R. On the other hand, the E_a for the CO formation is calculated to be 0.55 eV at U_0=−0.89 V vs. RHE. Accordingly, the E_a becomes 0.99(±0.18) eV at zero bias. This E_a decreases to 0.79(±0.10) and 0.69(±0.06) eV at −0.4 and −0.6 V vs RHE, respectively, and these barriers can lead to fast kinetics at room temperature[3].

Figure S3. CI-NEB calculation results for the first (COOH formation) and second (CO formation) protonation steps.

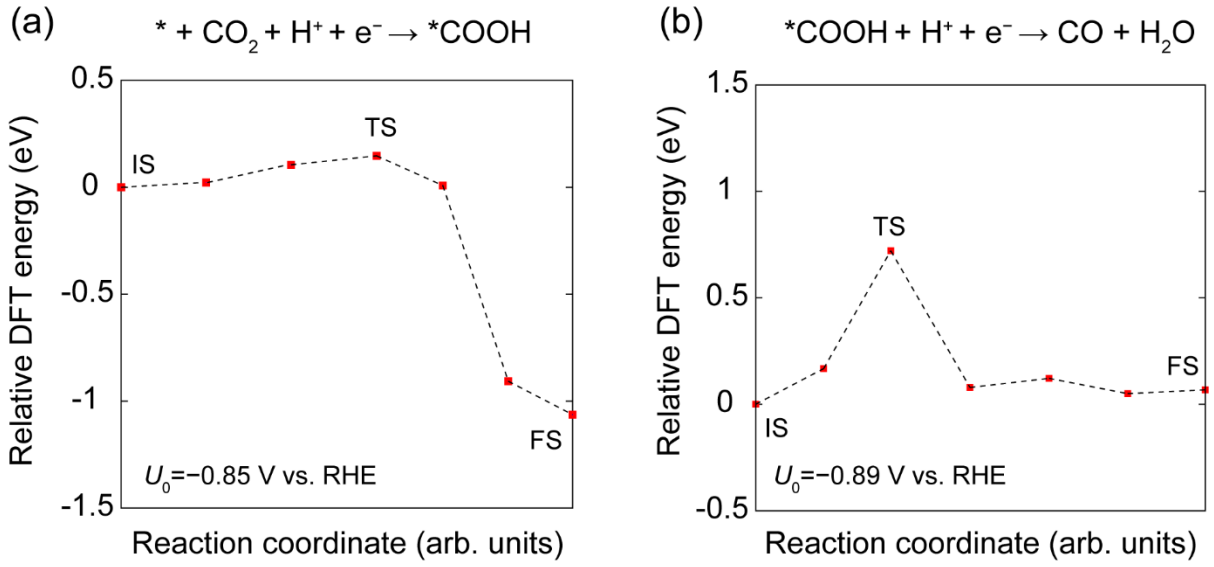

Figure S4. Atomic structures of the (a) initial (IS), (b) transition (TS), and (c) final (FS) states involved in COOH formation.

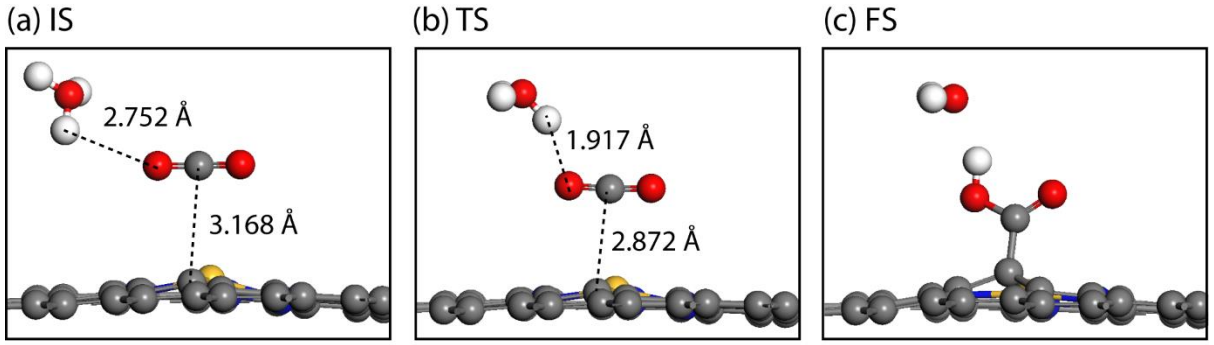

Figure S5. Atomic structures of the (a) initial (IS), (b) transition (TS), and (c) final (FS) states involved in CO formation.

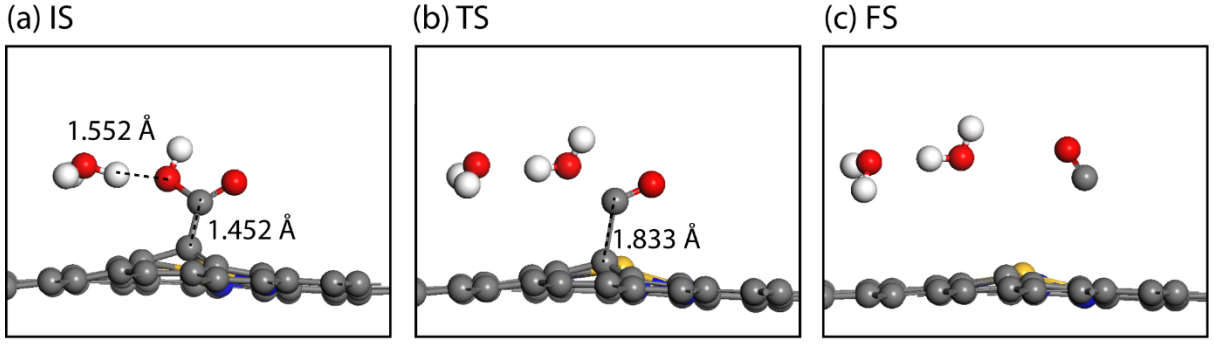

Figure S6. First three protonation steps on the Zn site in a ZnN_4 moiety.

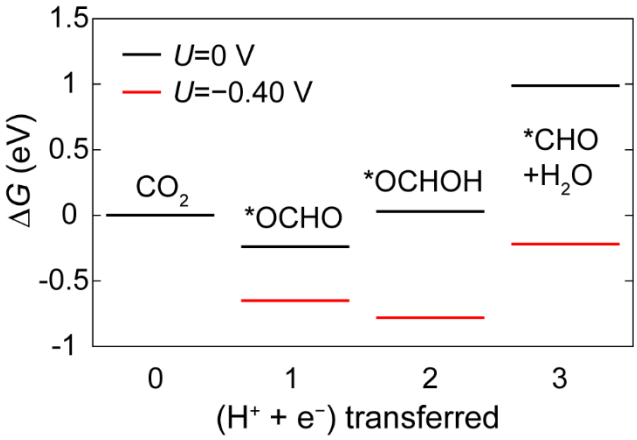

Figure S7. DOSs of the C_{NN} and C of *COOH for the in-plane component of 2p states towards the divacancy site (a) before and (b) after *COOH adsorption in a N_3C moiety.

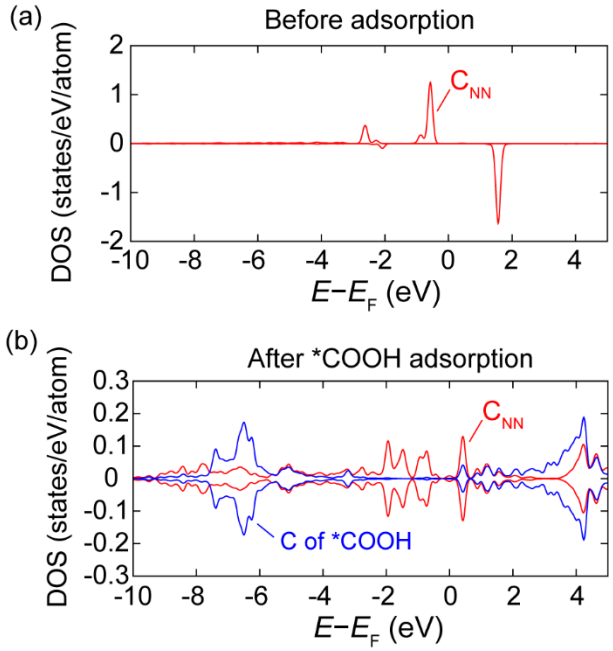

References

[1] S. A. Akhade, N. J. Bernstein, M. R. Esopi, M. J. Regula, and M. J. Janik, *Catal. Today* **2017**, *288*, 63-73.

[2] W. Luo, X. Nie, M. J. Janik, and A. Asthagiri, *ACS Catal*. **2016**, *6*, 219-229.

[3] J. H. Montoya, C. Shi, K. Chan, and J. K. Nørskov, *J. Phys. Chem. Lett.* **2015**, *6*, 2032-2037.